Electronic Supplementary Information

Multifunctional fluorescent Eu-MOF probe for tetracycline antibiotics and dihydrogen phosphate sensing and latent fingerprints visualization

Theanchai Wiwasuku[a,e], Adulvit Chuaephon[b], Theerapong Puangmali[b], Jaursup Boonmak[a*], Somlak Ittisanronnachai[c], Vinich Promarak[d], and Sujittra Youngme[a]

[a]*Materials Chemistry Research Center and Center of Excellence for Innovation in Chemistry, Department of Chemistry, Faculty of Science, Khon Kaen University, Khon Kaen 40002, Thailand.*

[b]*Department of Physics, Faculty of Science, Khon Kaen University, Khon Kaen 40002, Thailand.*

[c]*Frontier Research Center (FRC), Vidyasirimedhi Institute of Science and Technology, Rayong 21210, Thailand.*

[d]*Department of Materials Science and Engineering, School of Molecular Science and Engineering, Vidyasirimedhi Institute of Science and Technology, Rayong 21210, Thailand.*

[e]*Functional Materials and Nanotechnology Center of Excellence, Walailak University, Nakhon Si Thammarat, 80160, Thailand.*

[*] *E-mail: jaursup@kku.ac.th*

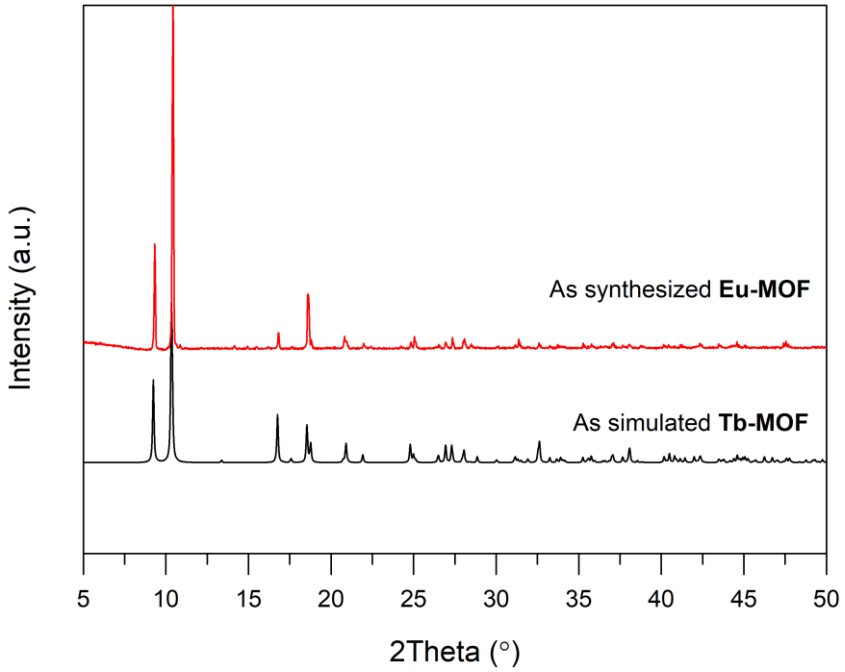

Fig. S1. PXRD of as simulated **Tb-MOF** and **Eu-MOF**.

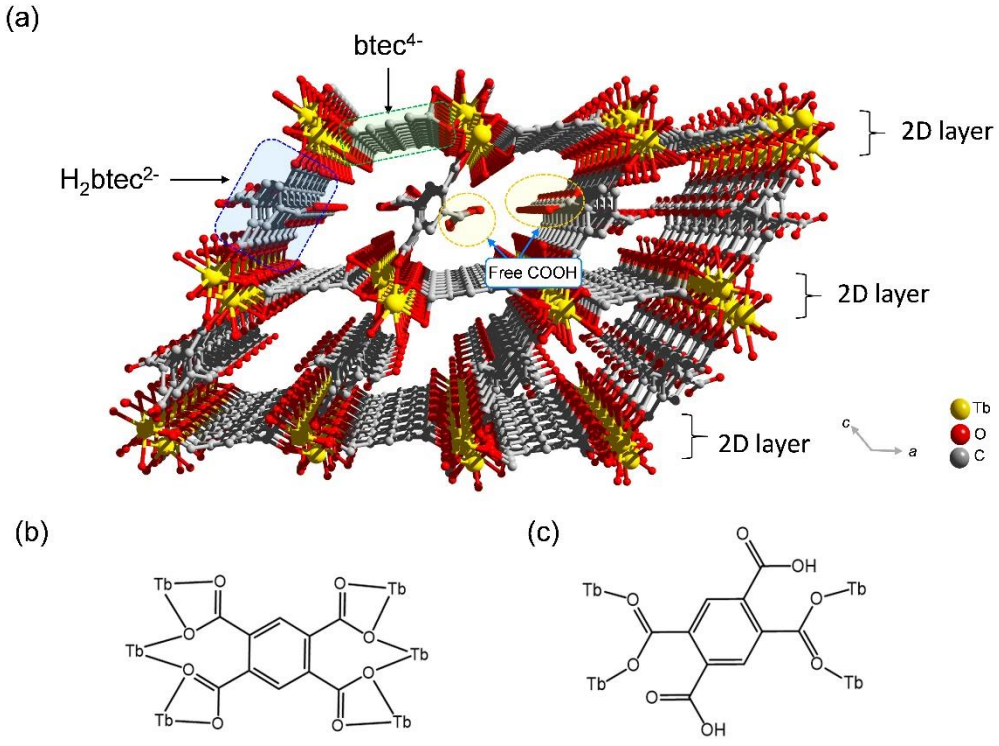

Fig. S2 (a) View along the *b* axis of the three-dimensional network. Coordination modes of (b) $btec^{4-}$ and (c) H_2btec^{2-} ligands in **Tb- MOF**.

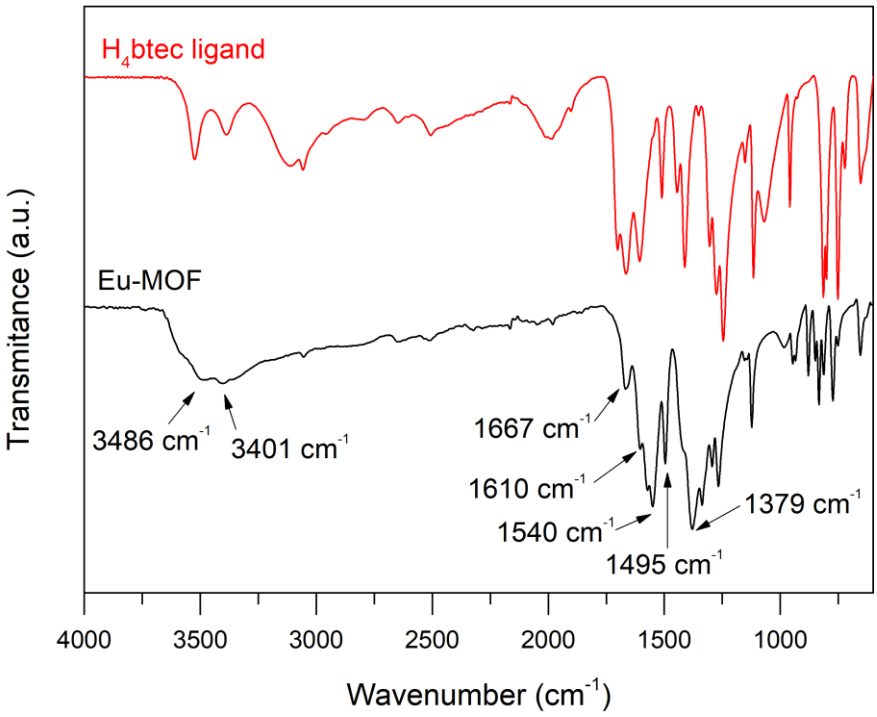

Fig. S3 FT-IR spectrum of H_4btec ligand and **Eu-MOF**.

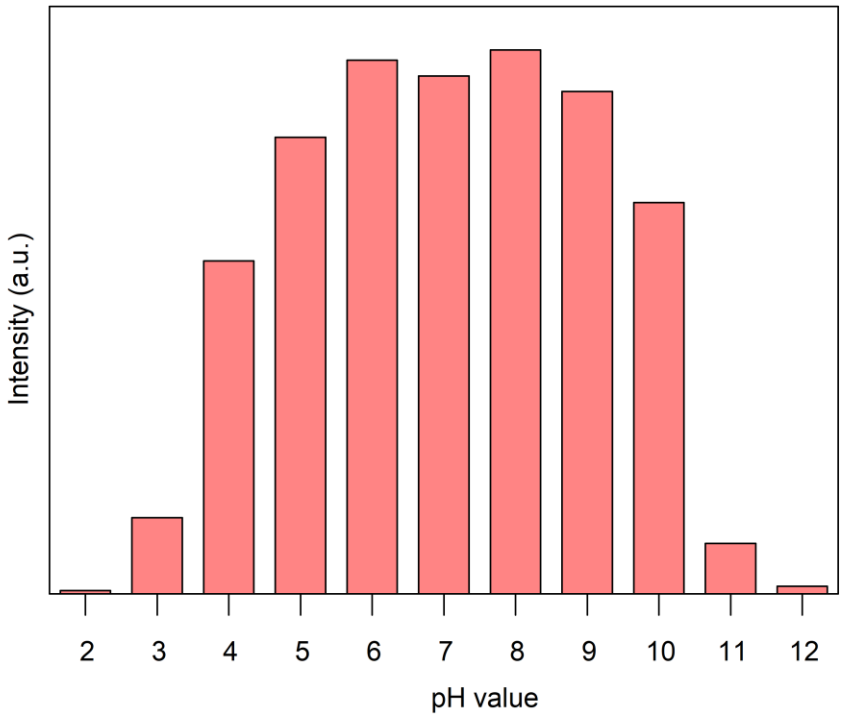

Fig. S4 Fluorescent intensity at 616 nm of **Eu-MOF** at pH 2-12.

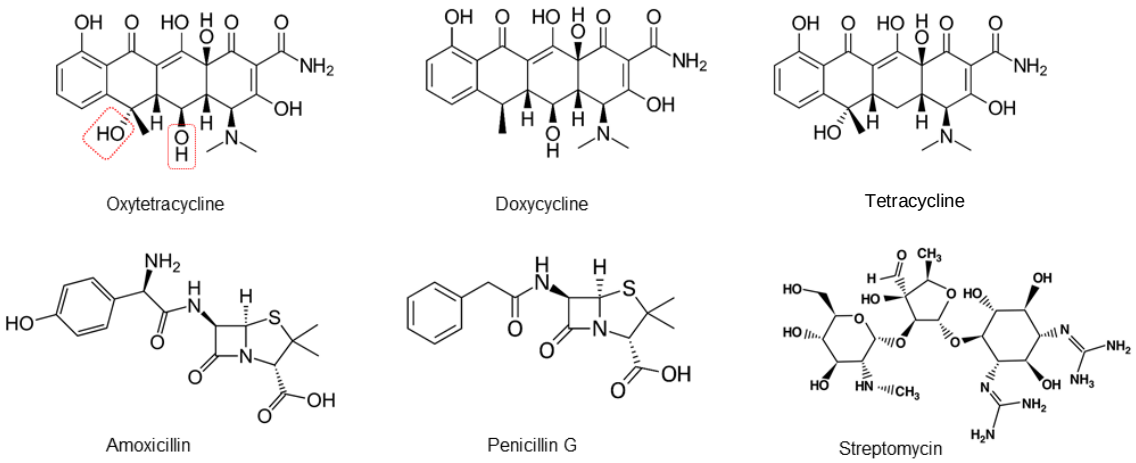

Fig. S5 Chemical structures of the studied antibiotics.

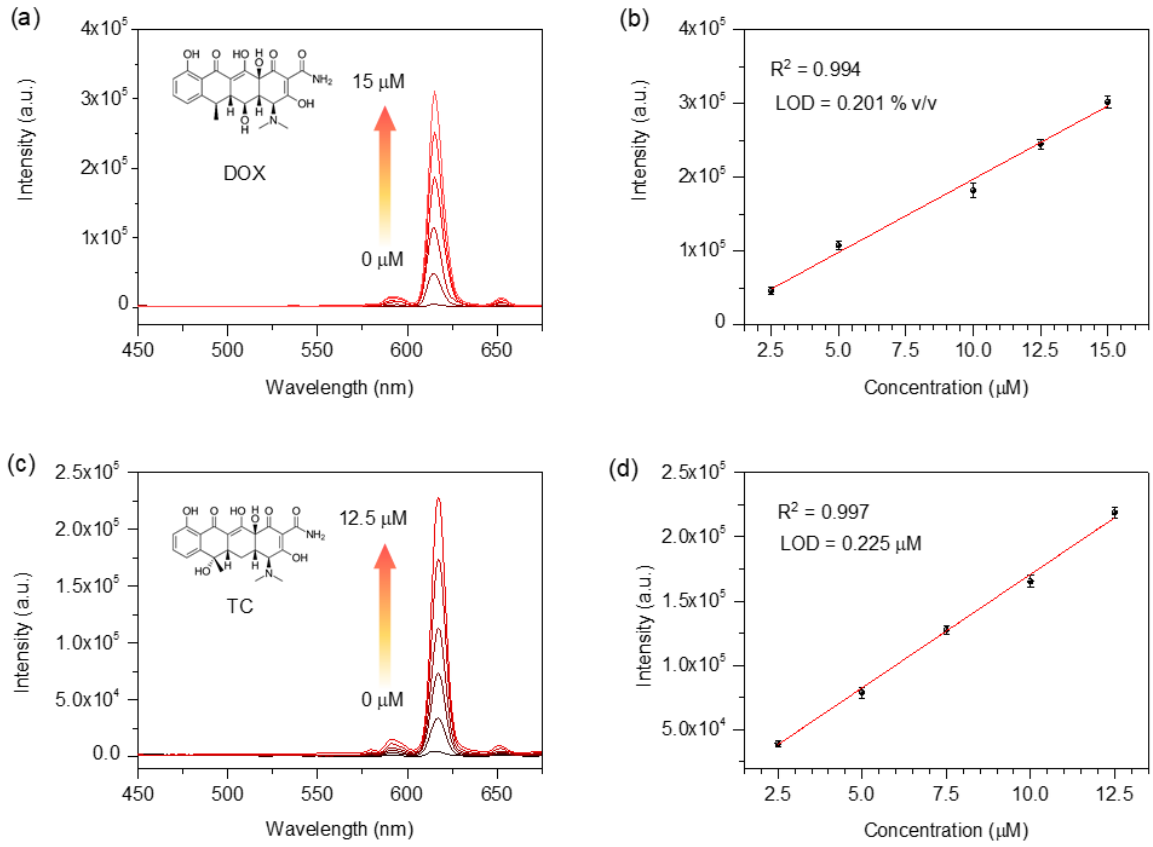

Fig. S6 (a and c) Fluorescent spectrum of **Eu-MOF** upon addition of DOX and TC at various concentrations. (b and d) plot of the fluorescent intensity of **Eu-MOF** at 616 nm as a function of TCs concentrations.

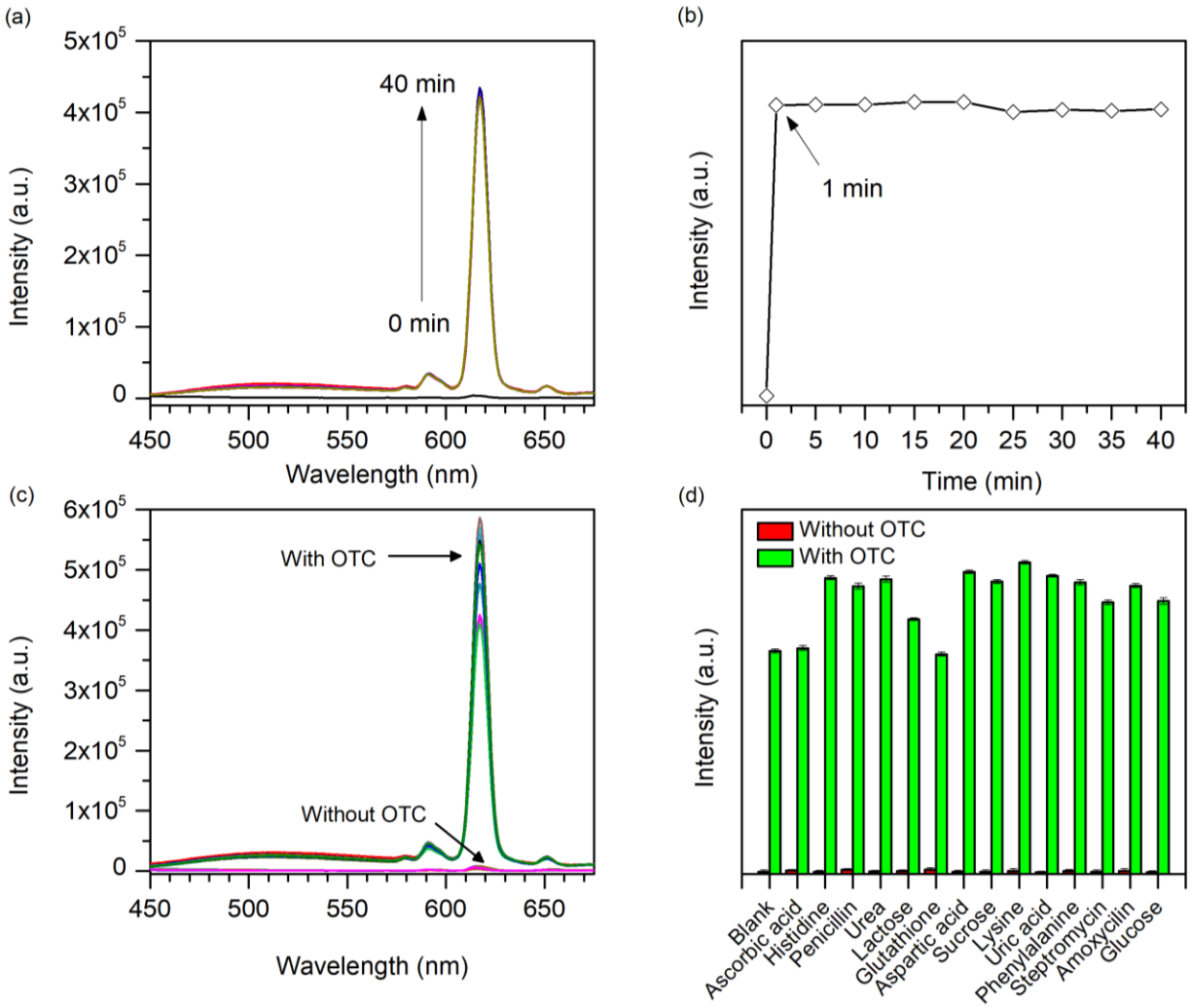

Fig. S7 (a) Fluorescent spectra and (b) intensity at 616 nm for **Eu-MOF** in the presence of OTC (25 μM) as a function of time. (c) Fluorescent spectra and (d) intensity at 616 nm of **Eu-MOF** in the presence of OTC (25 μM) with various interference chemicals (25 μM).

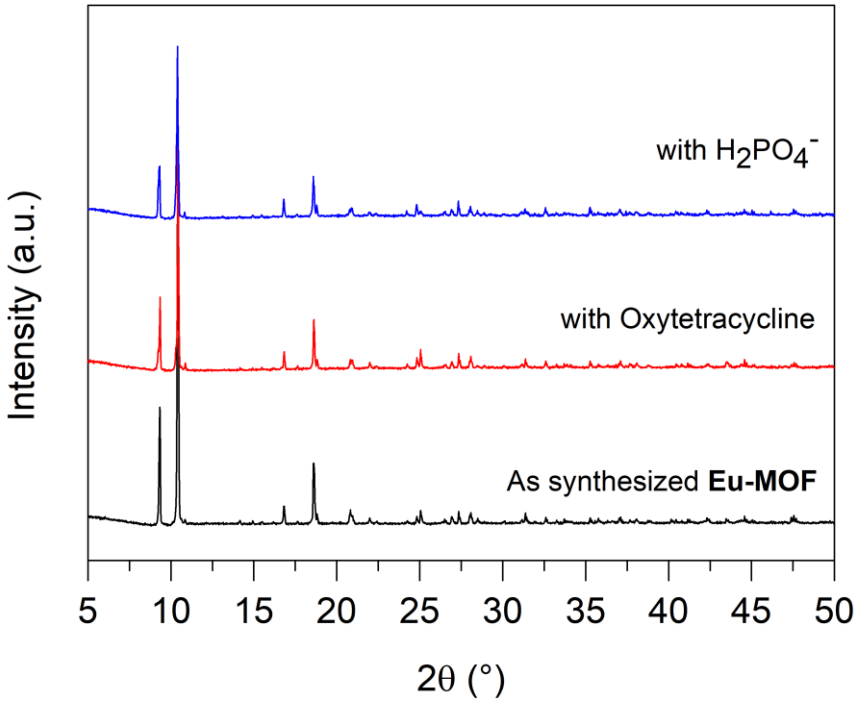

Fig. S8 PXRD pattern of as-synthesized **Eu-MOF, Eu-MOF** treated with OTC, and **Eu-MOF** treated with $H_2PO_4^-$.

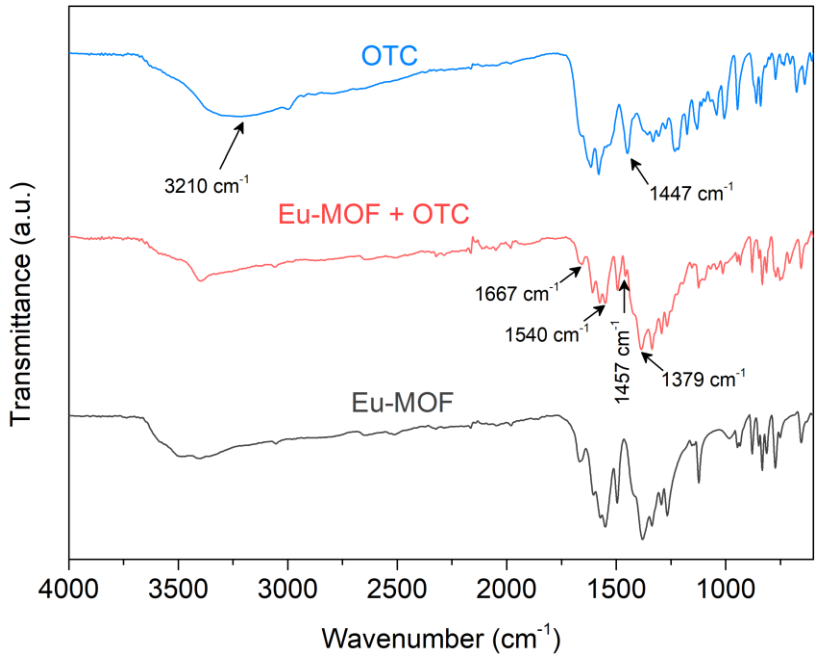

Fig. S9 FT-IR spectra of OTC, **Eu-MOF+OTC**, and **Eu-MOF**.

Table S1 The selected fluorescent sensors for tetracyclines (TCs) detection.

Sensor	Solvent media	Fluorescent response	TCs type	Detection range	LOD	Ref.
MOFs						
CDs@HZIF-8	Water	Ratiometric	OTC	0.5-40 μM	29.46 nM	[1]
		sensing	TC	0.5-50 μM	6.56 nM	
Tb-MOF	Water	Ratiometric	OTC	0.2- 43.0 μM	43 nM	[2]
		sensing	TC	0.12-20.7 μM	18 nM	
			DOX	0.31-42.0 μM	45 nM	
NH_2-MIL-53(Al)	Water	Turn-off	OTC	0-86.67 μM	62.05 nM	[3]
			TC	0-72.33 μM	26.16 nM	
			DOX	0-66.67 μM	40.36 nM	
Tb-MOF	Water	Turn-off	OTC	0-50 μM	1.95 nM	[4]
			TC	0-50 μM	2.77 nM	
Cd-MOF	Water	Turn-off	OTC	0-30 μM	13.53 μM	[5]
			TC	0-30 μM	8.97 μM	
			DOX	0-30 μM	11.76 μM	
In-MOF	Water	Turn-off	OTC	0-30 μM	300 nM	[6]
			TC	0-30 μM	280 nM	
Zn-MOF	Water	Turn-on	OTC	0.02–13 μM	17 nM	[7]
Eu-In-BTEC	Water	Turn-on	DOX	0.5-2.5 μM	47 nM	[8]
Eu-MOF	Water	Turn-on	OTC	2.5-15 μM	78 nM	**This**
			TC	2.5-12.5 μM	225 nM	**work**
			DOX	2.5-15 μM	201 nM	
Other materials						
Cu-CDs	Water	Turn-off	OTC	2–44 μM	160 nM	[9]
			TC	2-32 μM	170 nM	
AuNCs	Water	Turn-on	OTC	0.375–12.5 μM	150 nM	[10]
BNQD/Eu^{3+}	Water	Turn-off	OTC	0-50 μM	104 nM	[11]
			TC	0-50 μM,	19 nM	
			DOX	0-50 μM	28 nM	

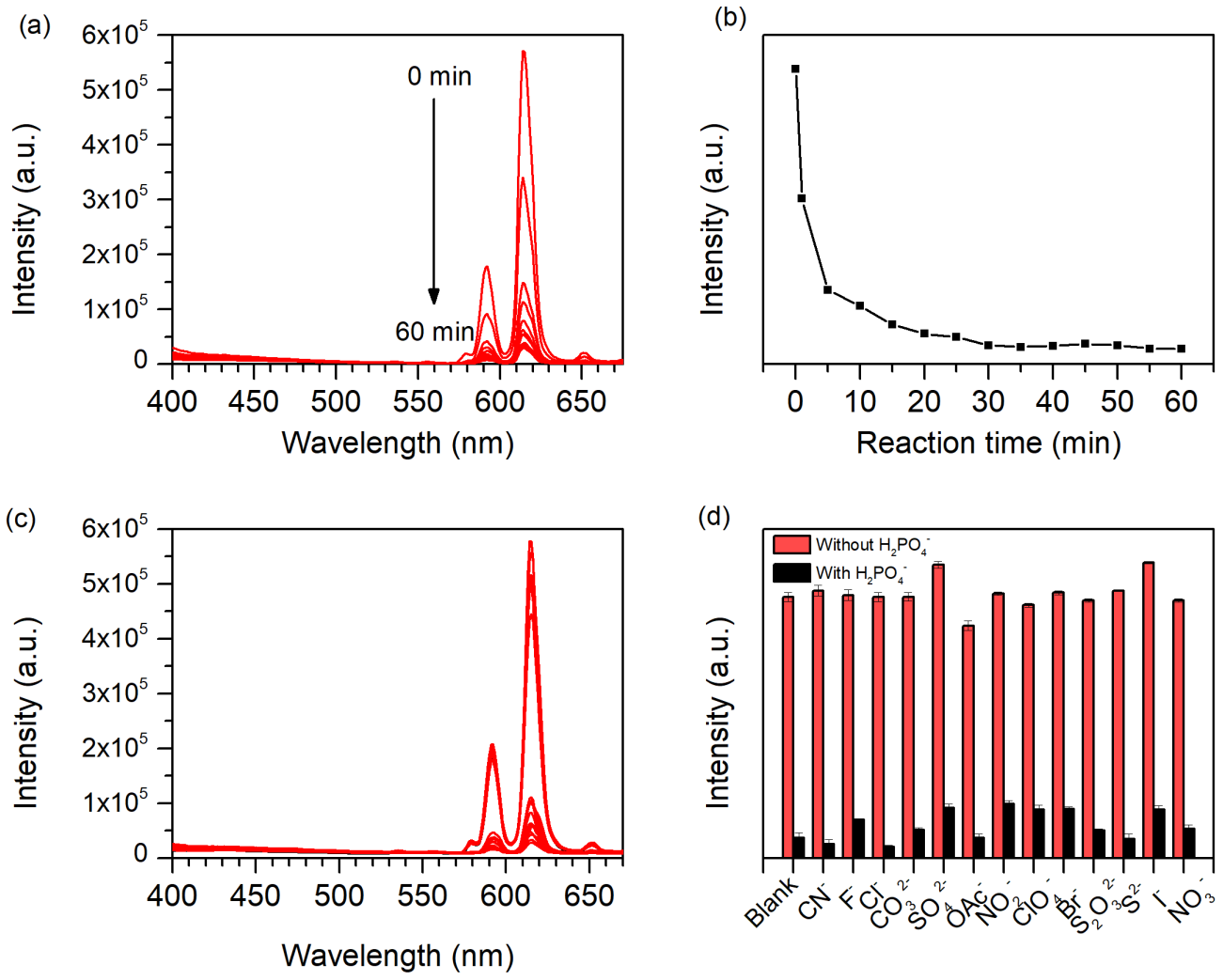

Fig. S10 (a) Fluorescent spectra and (b) intensity at 616 nm for **Eu-MOF** in the presence of $H_2PO_4^-$ (50 μM) as a function of time. (c) Fluorescent spectra and (d) intensity at 616 nm of **Eu-MOF** in the presence of $H_2PO_4^-$ (50 μM) with various interference chemicals (50 μM).

Table S2 The selected fluorescent sensors for $H_2PO_4^-$ detection.

MOF	Solvent media	Fluorescent response	Detection range	LOD	Ref.
MOFs					
Zn-DMBI	MeOH	Turn-on	0-8 μM	1.3 μM	[12]
Pyrene tagged UiO-66-NH2	DI	Turn-on	-	0.73 μM	[13]
Zn-MOF	CH_3OH/DI	Turn-off	-	3.903 μM	[14]
Eu-MOF	DI	Turn-off	2.5-15 μM	0.70 μM	**This work**
Other materials					
Tb complex	DI	Turn-off	-	4.82 μM	[15]
2-(2′-tosylamido phenyl)thiazole	EtOH	Turn-off	-	1 μM	[16]
Zn coordinated pyridine based sensor	CH_3CN	Turn-off	-	3.44 μM	[17]

References

[1] Y. Li, Y. Wang, P. Du, L. Zhang, Y. Liu, X. Lu, Fabrication of carbon dots@hierarchical mesoporous ZIF-8 for simultaneous ratiometric fluorescence detection and removal of tetracycline antibiotics. *Sens. Actuators B Chem.*, 358, **2022**, 131526.

[2] R. Li, W. Wang, E.-S. M. El-Sayed, K. Su, P. He, and D. Yuan, Ratiometric fluorescence detection of tetracycline antibiotic based on a polynuclear lanthanide metal–organic framework. *Sens. Actuators B Chem.*, 330, **2021,** 129314.

[3] C. Li, L. Zhu, W. Yang, X. He, S. Zhao, X. Zhang, W. Tang, J. Wang, T. Yue, Z. Li, Amino functionalized Al MOF for fluorescent detection of tetracyclines in milk. *J. Agric. Food Chem.*, 67 (4), **2019**, 1277-1283.

[4] C. Li, C. Zeng, Z. Chen, Y. Jiang, H. Yao, Y. Yang, W.- T. Wong, *J. Hazard. Mater.*, 384, **2020**, 121498.

[5] H.-H. Wang, Y. Zhang, D.-B. Yang, L. Hou, Z.-Y. Li, Y.-Y. Wang, Fluorine-Substituted Regulation in Two Comparable Isostructural Cd(II) Coordination Polymers: Enhanced

Fluorescence Detection for Tetracyclines in Water, *Cryst. Growth Des.*, **2021**, 21, 2488−2497.

[6] Q. Liu, D. Ning, W.J. Li, X.M. Du, Q. Wang, Y. Li, W. J. Ruan, Metal-organic framework-based fluorescent sensing of tetracycline-type antibiotics applicable to environmental and food analysis, *Analyst*, 144**, 2019**, 1916–1922.

[7] J. Chen, F. Xu, Q. Zhang, S. Li, X. Lu, Tetracycline antibiotics and NH_4^+ detection by Zn–organic framework fluorescent probe, *Analyst*, **2021**, 146, 6883–6892.

[8] L. Yu, H. Chen, J. Yue, X. Chen, M.i Sun, J. Hou, K. A. Alamry, H. M. Marwani, X. Wang, S.Wang, Europium metal-organic framework for selective and sensitive detection of doxycycline based on fluorescence enhancement. *Talanta*, **2020**, 207, 120297.

[9] J. Guo, W. Lu, H. Zhang, Y. Meng, F. Du, S. Shuang, C. Dong, Copper doped carbon dots as the multifunctional fluorescent sensing platform for tetracyclines and pH. *Sens. Actuators B Chem.*, 330, **2021**, 129360.

[10] S. Xu, X. Li, Y. Mao, T. Gao, X. Feng, X. Luo, Novel dual ligand co functionalized fluorescent gold nanoclusters as a versatile probe for sensitive analysis of Hg^{2+} and oxytetracycline. *Anal. Bioanal. Chem.*, 408 (11), **2016**, 2955-2962.

[11] K. Yang, P. Jia, J. Hou, T. Bu, X. Sun, Y. Liu, L. Wang, Innovative dual emitting ratiometric fluorescence sensor for tetracyclines detection based on boron nitride quantum dots and europium ions. *ACS Sustainable Chem. Eng.*, 8 (46), **2020**, 17185-17193.

[12] J. Swati, J. N. Moorthy, Zwitterionic Luminescent 2D Metal−Organic Framework Nanosheets (LMONs): Selective Turn-On luorescence Sensing of Dihydrogen Phosphate. *Inorg. Chem.*, 61, **2022**, 3942−3950.

[13] R. Dalapati, S. Biswas, Chemical Post-Synthetic Modification of a Metal-Organic Framework with Fluorescent-Tag for Dual Naked-Eye Sensing in Aqueous Medium. *Sensors Actuators B. Chem.*, 239, **2017**, 759–767.

[14] R. Naskar, K. Bhanja, A. K.; Paul, S.; Pal, K.; Sinha, C. Trace Quantity Detection of $H_2PO_4^-$ by Fluorescent Metal−Organic Framework (F-MOF) and Bioimaging Study. *Cryst. Growth Des.*, 20, **2020**, 6453–6460.

[15] Y. Su, D. Zhang, P. Jia, W. Gao, Y. Li, Z. Bai, X. Liu, Q. Deng, J. Xu, C. Yang, Highly Selective and Sensitive Long Fluorescence Lifetime Polyurethane Foam Sensor Based on Tb-Complex as Chromophore for the Detection of $H_2PO_4^-$ in Water. *Spectrochim. Acta Part A Mol. Biomol. Spectrosc.*, 217, **2019**, 86–92.

[16] M. An, B.-Y. Kim, H. Seo, A. Helal, H.-S. Kim, Fluorescence Sensor for Sequential Detection of Zinc and Phosphate Ions. *Spectrochim. Acta - Part A Mol. Biomol. Spectrosc.*, 169, **2016**, 87–94.

[17] X. Feng, Y. Fu, J. Jin, J. Wu, A Highly Selective and Sensitive Fluorescent Sensor for Relay Recognition of Zn^{2+} and $HSO_4^{2-}/H_2PO_4^-$ with "on-off" Fluorescent Responses. *Anal. Biochem., 563*, **2018**, 20–24.

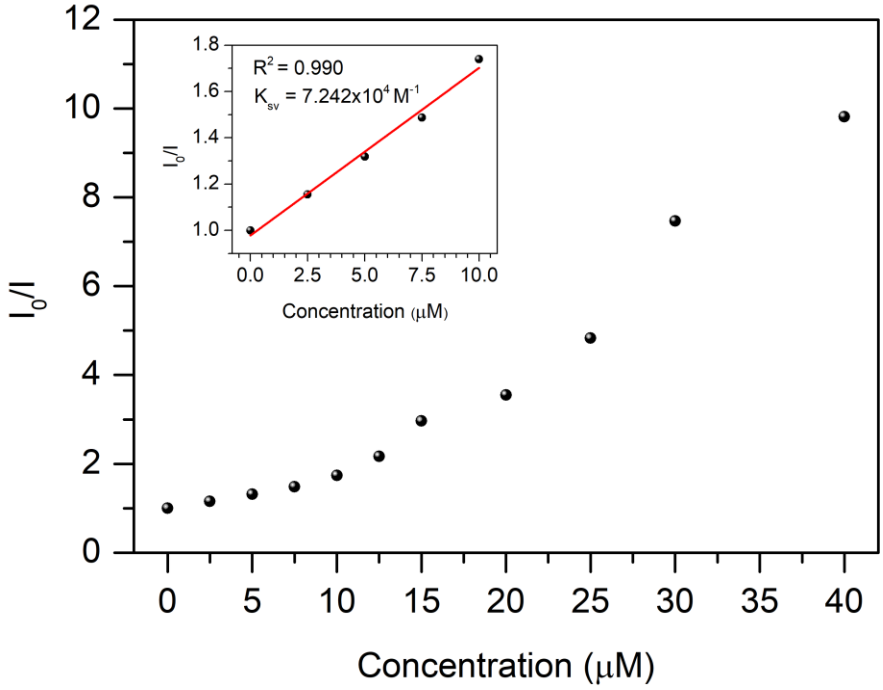

Fig. S11 Stern-Volmer plot for **Eu-MOF** in the presence of $H_2PO_4^-$ at various concentrations. The inset figure displays a linear regression curve for 0-10 μM $H_2PO_4^-$.

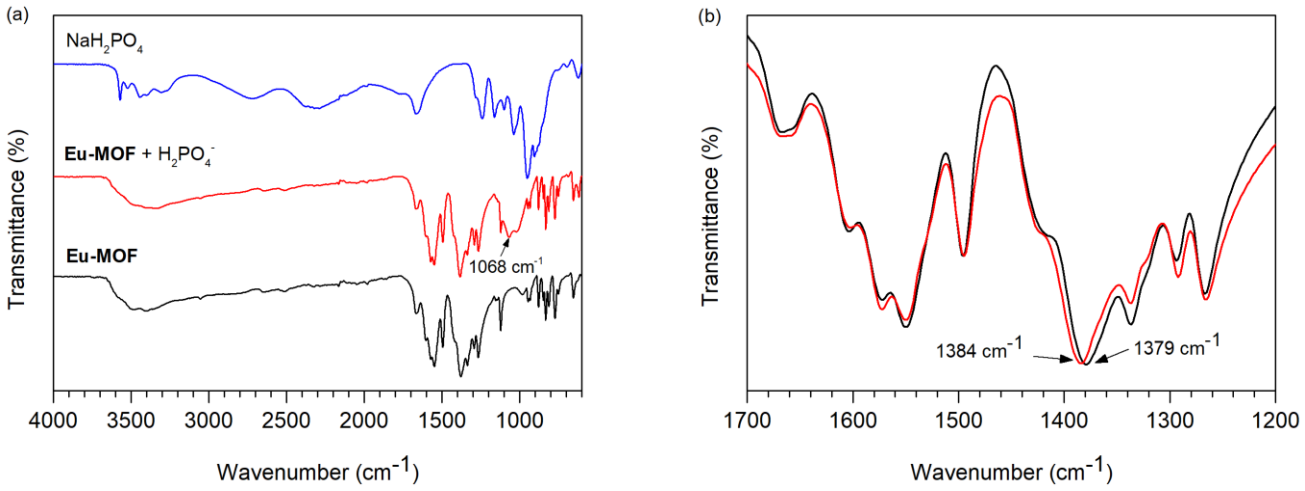

Fig. S12 (a) FT-IR spectrum of NaH_2PO_4, **Eu-MOF** and **Eu-MOF** + $H_2PO_4^-$. (b) Magnified FT-IR spectrum of **Eu-MOF** (black line) and **Eu-MOF** + $H_2PO_4^-$ (red line).

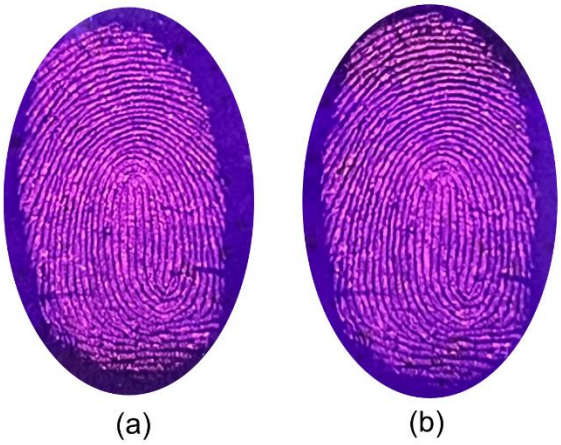

Fig. S13 Photostability image of **Eu-MOF** developed LFPs after UV (365 nm) irradiation for (a) 0 hr and (b) 7 hrs.

Fig. S14 Long-term stability image of **Eu-MOF** developed LFPs after storage for (a) 0 day, (b) 7 days, and (c) 30 days.

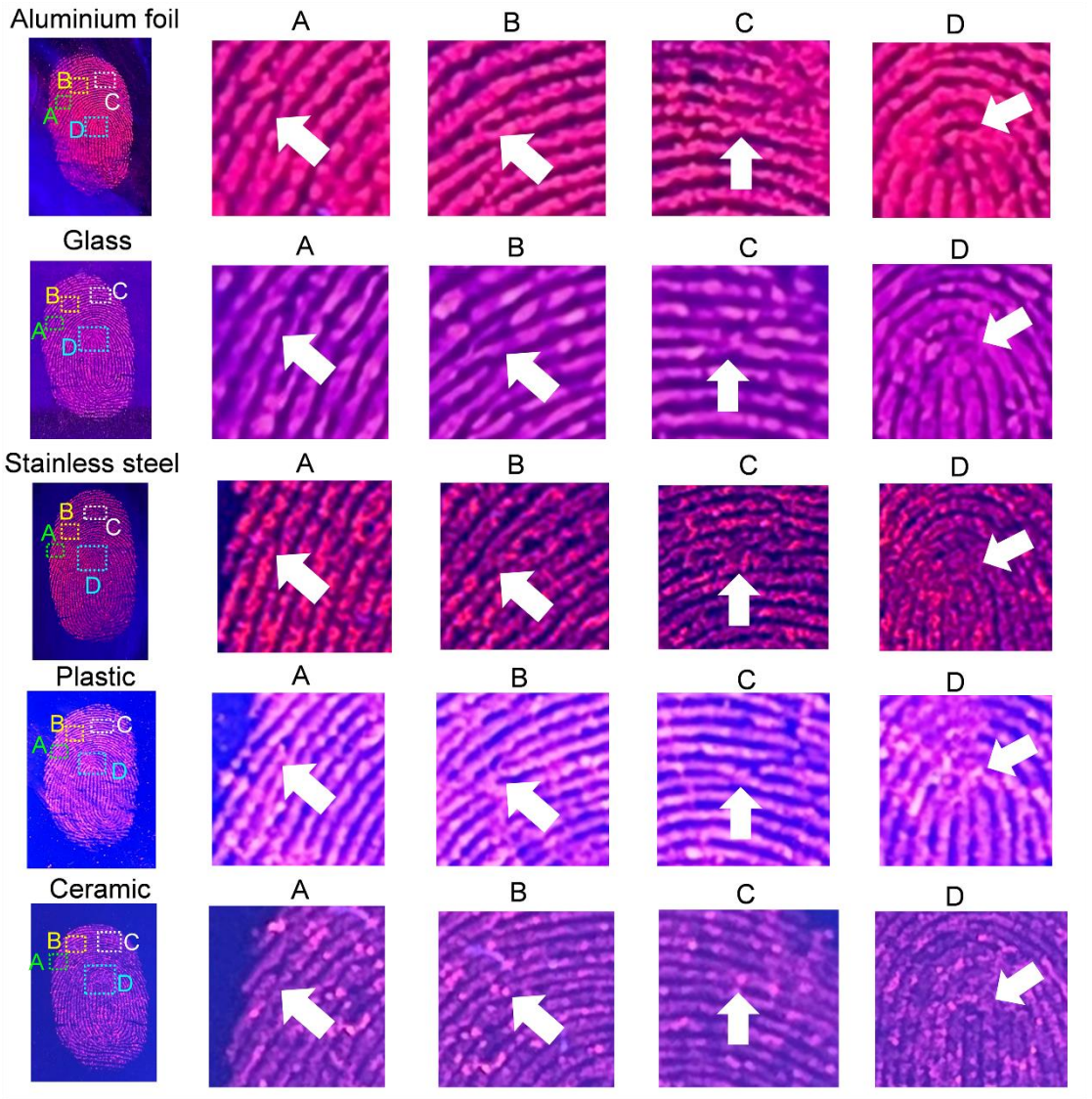

Fig. 15 Enlarged images of latent fingerprints developed with materials on different substrates under UV light. The magnified fingerprint details show (A) termination, (B) bifurcation, (C) crossover, and (D) core point.